5. THE ARCTIC—J. Richter-Menge

a. Overview

In 2008 there continued to be broad evidence of the impact of a general, Arctic-wide warming trend in surface air temperatures over land, apparent since the mid-1960s. Record-setting summer (JJA) air temperatures were observed throughout Greenland. The northern region of Greenland and adjacent areas of Arctic Canada experienced a particularly intense melt season, even though there was an abnormally cold winter across Greenland's southern half. On land there was a continued Arctic-wide trend toward a shorter snow season, highlighted by the shortest snow cover duration on record (beginning in 1966) in the North American Arctic. There has been a general increase in land-surface temperatures and in permafrost temperatures during the last several decades throughout the Arctic region. New permafrost data from Russia show striking similarity to observations made in Alaska, with permafrost temperature typically having increased by 1° to 2°C in the last 30 to 35 years. One of the most dramatic signals of the general warming trend was the continued significant reduction in the extent of the summer sea-ice cover and, importantly, the decrease in the amount of relatively older, thicker ice. The extent of the 2008 summer sea-ice cover was the second-lowest value of the satellite record (beginning in 1979) and 36% below the 1979–2000 average. Summer temperature anomalies in the ocean surface layer remained relatively high, reaching above +3°C in the Beaufort Sea. Significant losses in the mass of ice sheets and the area of ice shelves continued, with several fjords on the northern coast of Ellesmere Island being ice free for the first time in 3,000–5,500 years.

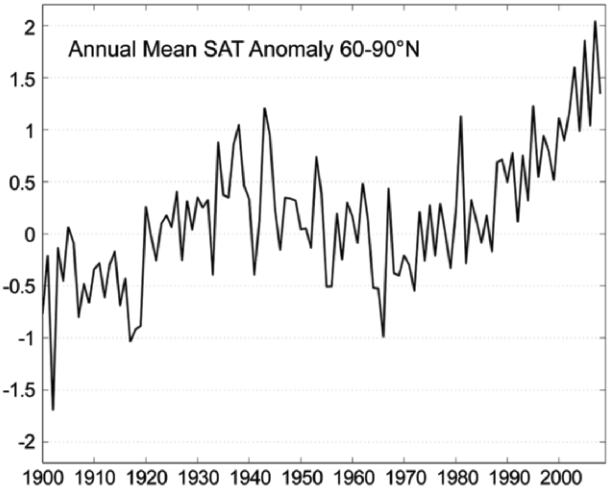

Fig. 5.1. Arctic-wide annual averaged surface air temperature anomalies (60°–90°N) based on land stations north of 60°N relative to the 1961–90 mean. From the CRUTEM 3v dataset (available online at www.cru.uea.ac.uk/cru/data/temperature/). Note: this curve does not include marine observations.

Documented signs of connectivity between the various elements of the Arctic system are beginning to emerge. For instance, a comparison of ocean surface temperatures during the summer of 2007 and 2008 provides clear evidence that the timing in the loss of the summer sea-ice cover plays a significant role in determining the magnitude and distribution of ocean surface temperatures. It is apparent that the heating of the ocean in areas of extreme summer sea-ice loss is directly impacting surface air temperatures over the Arctic Ocean, where surface air temperature anomalies reached an unprecedented +5°C during October through December 2008. Direct observations confirm model predictions that the effects of the retreating sea ice influence the temperature and vegetation of adjacent lands. Temporal analyses generally show that within a specific region, periods of lower sea-ice concentration are correlated with higher land-surface temperatures and an increase in the amount of live green vegetation in the summer.

b. Atmosphere—J. Overland, M. Wang, and J. Walsh

The annual mean Arctic temperature for 2008 was the fourth-warmest year for land areas since 1990 (Fig. 5.1). This continued the twenty-first century positive Arctic-wide SAT anomalies of greater than 1.0°C, relative to the 1961–90 reference period. The mean annual temperature for 2008 was cooler than 2007, coinciding with cooler global and Pacific temperatures (Hansen et al. 2009).

Similar to the previous years of the twenty-first century, in 2008 the spatial extent of positive SAT anomalies in winter and spring of greater than +1°C was nearly Arctic-wide (Fig. 5.2a), in contrast with more regional patterns in the twentieth century (Chapman and Walsh 2007). The exception was the Bering Sea/southwestern Alaska, which experienced a fourth-consecutive cold or average winter associated with a strong negative PDO as 2008 came to a close.

The summer of 2008 ended with nearly the same extreme minimum sea-ice extent as in 2007, characterized by extensive areas of open water (see section 5d). This condition allows extra heat to be absorbed by the ocean from longwave and solar radiation throughout the summer season, which is then released back to the atmosphere the following autumn (Serreze et al. 2009). As a result, during October through December 2008 SAT anomalies

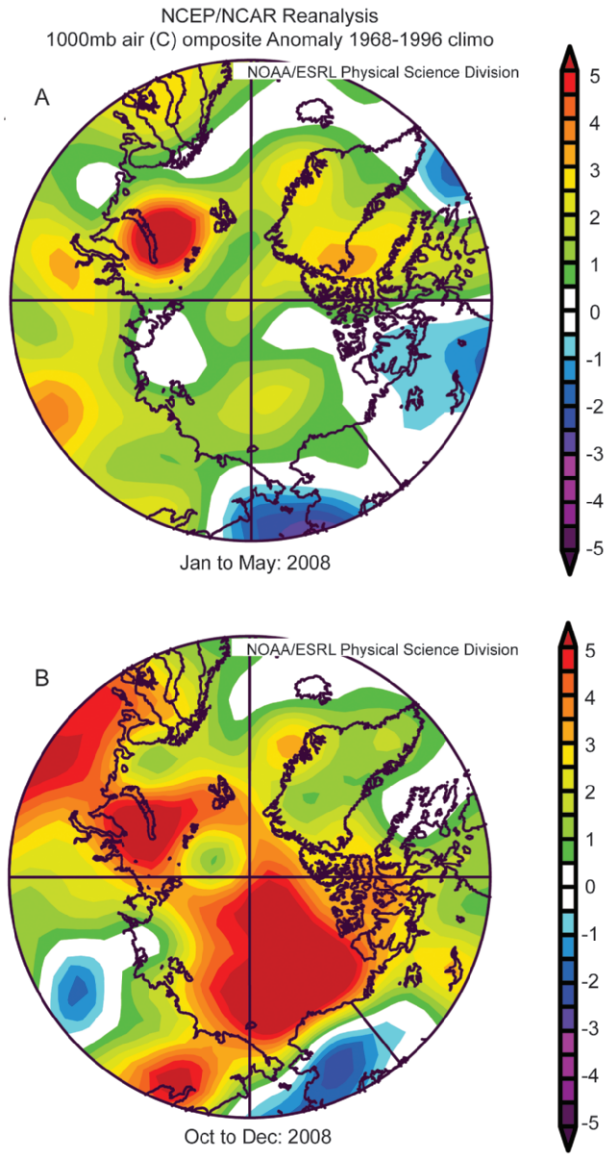

Fig. 5.2. Near-surface air temperature anomalies for (a) Jan–May 2008 and (b) Oct through Dec 2008. Anomalies are relative to 1968–96 mean. Data are from the NCEP–NCAR reanalysis through the NOAA/ Earth Systems Research Laboratory, generated online at www.cdc.noaa.gov.

remained above an unprecedented +5°C across the central Arctic (Fig. 5.2b).

The climate of the Arctic is influenced by repeating patterns of SLP that can either dominate during individual months or represent the overall atmospheric circulation flow for an entire season. 2008 continued twenty-first-century conditions where both the types of patterns and their frequency have shifted in comparison to the twentieth century. The main pattern of primarily zonal winds is known as the Arctic Oscillation. A second more meridional wind pattern that is more prevalent in the twenty-first century is known as the Arctic Warm pattern (Wu et al. 2006; Overland et al. 2008). The AW pattern has anomalous high SLP pressure on the North American side of the Arctic and low SLP on the Eurasian side, and it implies increased transport of heat into the central Arctic Ocean (e.g., Fig. 5.3). 2007 exhibited an unusually persistent positive AO pattern in the winter and AW pattern in all summer months, which helped to support the major 2007 summer reduction in sea-ice extent (Overland et al. 2008). 2008 was more typical of past patterns, characterized by month-to-month variability in the presence of these climate patterns, with no single pattern showing seasonal dominance.

There is evidence that by creating a new major surface heat source, the recent extreme loss of summer sea-ice extent is having a direct feedback effect on the general atmospheric circulation into the winter season (Francis et al. 2009). Fall air temperature anomalies of greater than +1.0°C were observed well up into the troposphere (Fig. 5.4a), when averaged over 2003–08 relative to a 1968–96 base period. The

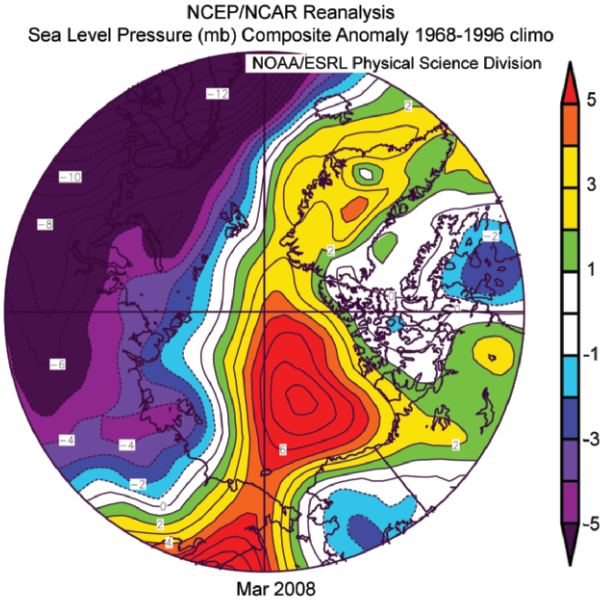

Fig. 5.3. An example of a positive AW pattern of SLP anomalies from Mar 2008. Purple/blue regions have relative low SLP and orange regions have high SLP. Anomalous winds tend to blow parallel to the contour lines, creating a flow from north of eastern Siberia across the North Pole. The orientation of the pressure dipole can shift; other examples have the anomalous geostrophic wind flow coming from north of the Bering Strait or Alaska. Data are from the NCEP–NCAR reanalysis available online at www.cdc.noaa.gov.

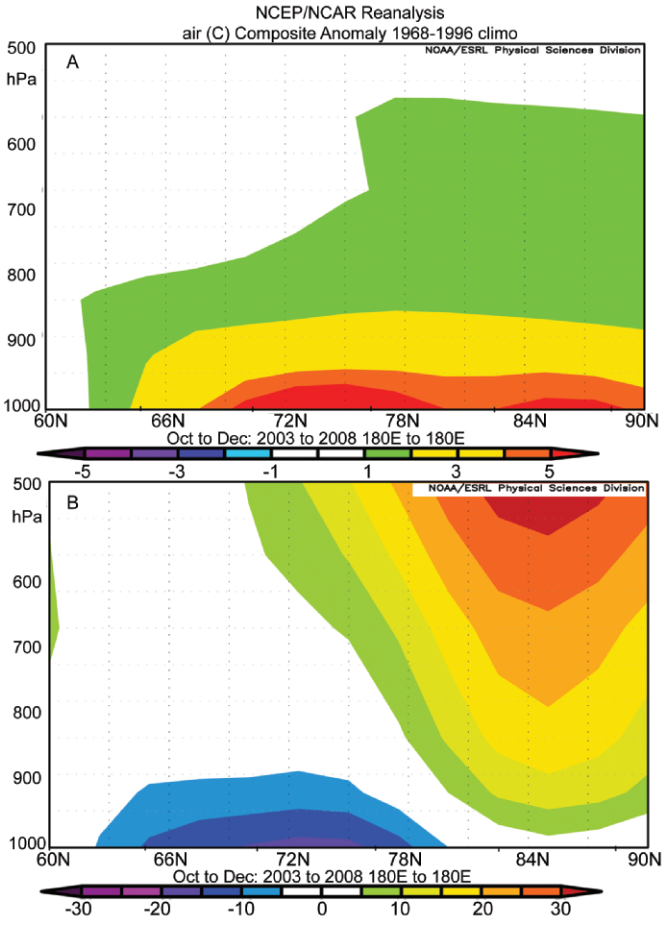

Fig. 5.4. Vertical cross section from 60° to 90°N along 180° longitude averaged for Oct–Dec 2003 through 2008 (years for which summertime sea-ice extent fell to extremely low values) for (a) air temperature and (b) geopotential height. Data are from the NCEP–NCAR reanalysis available online at www.cdc.noaa.gov.

higher temperatures in the lower troposphere increase the atmospheric geopotential thickness and raise upper-air geopotential heights above the Arctic Ocean (Fig. 5.4b). Increased geopotential heights north of 75°N weaken the normal north–south pressure gradient driving the polar vortex that creates west–east airflow aloft. In this sense, the effect of higher air temperatures in the lower troposphere is contributing to changes in the atmospheric circulation in the subarctic by reducing the potential impacts from the positive phase of the AO pattern, and perhaps contributing to the increased occurrence of the AW pattern.

c. Ocean—A. Proshutinsky, R. Krishfield, M. Steele, I. Polyakov, I. Ashik, M. McPhee, J. Morison, M.-L. Timmermans, J. Toole1, V. Sokolov, I. Frolov, E. Carmack, F. McLaughlin, K. Shimada, R. Woodgate, and T. Weingartner

1) Circulation

In 2008, the ocean surface circulation regime in the central Arctic was anticyclonic (clockwise) in winter and summer (Fig. 5.5). The intensity of motion was weaker than observed in 2007, consistent with changes in the observed sea level atmospheric pressure patterns (see section 5b). In winter the major flow stream removed sea ice from the Kara and Laptev Seas, while in the summer sea ice from the Canada Basin was transported toward the Fram Strait. Data from satellites and drifting buoys (Proshutinsky et al. 2009) indicate that the entire period of 1997–2008 has been characterized by a relatively stable anticyclonic ocean surface circulation regime. This circulation pattern was the result of a higher sea level atmospheric pressure over the Arctic Ocean, relative to the 1948–2008 mean, and the prevalence of anticyclonic winds. These conditions have significantly influenced the sea-ice cover, oceanic currents, and ocean freshwater and heat content.

2) Water temperature and salinity

Upper-ocean temperatures in summer 2008 were not quite as high as in the record-breaking summer of 2007. Although the position of the September ice edge did not change significantly in 2008 relative to 2007, the timing of ice retreat was different. Early ice retreat from the Beaufort

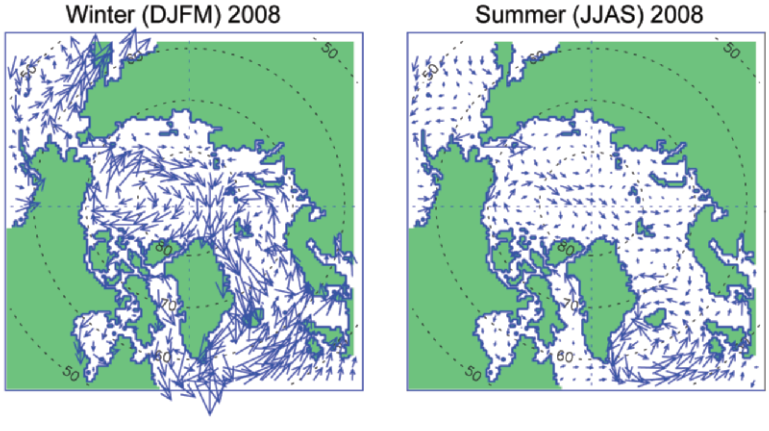

Fig. 5.5. Simulated circulation patterns of the upper-ocean wind-driven circulation in (left) winter and (right) summer in 2008. Both patterns are identified as anticyclonic (clockwise). The intensity of anticyclonic circulation in summer 2008 has reduced relative to 2007 (see Proshutinsky and Johnson 1997 for details).

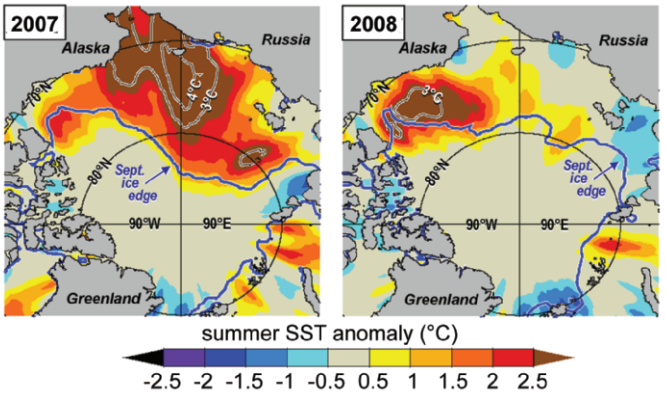

Fig. 5.6. Satellite-derived summer (JAS) SST anomalies (Reynolds et al. 2002) in (left) 2007 and (right) 2008, relative to the summer mean over 1982–2006. Also shown is the Sep mean ice edge (thick blue line).

Sea in 2008 led to anomalously high sea surface temperatures that exceeded even those in 2007 in this region (Fig. 5.6). However, ice retreat in the Chukchi and east Siberian Seas occurred relatively late in the summer, leading to near-normal or only slightly above-normal ocean warming (Fig. 5.6). This difference illustrates that the warming of the upper ocean is dependent not only on the position of the September ice edge but also on the time history of the ice cover over the summer. More specifically, ocean surface warming depends on the time history of atmospheric heat input to the sea surface, which depends both on atmospheric conditions (winds, clouds) and on the presence of the ice cover that acts to block this heat input (Steele et al. 2009, manuscript submitted to *J. Geophys. Res.*).

Changes in the AWCT varied regionally in 2008, reflecting temporal pulses in the Atlantic water flow volume, temperature, and salinity in the Fram Strait. The Atlantic water propagates cyclonically (counterclockwise) along the Arctic Ocean continental slope, entering the Arctic Ocean via the Fram Strait west of Spitsbergen and leaving the Arctic via the Fram Strait east of Greenland. Observations at a NABOS (http://nabos.iarc.uaf.edu/) mooring in the vicinity of Spitsbergen (Fig. 5.7) along the entry point of the AWCT showed that the monthly mean AWCT at 260 m reached a maximum of ~3.8°C in November–December 2006. Subsequently, the temperature at this location has declined or cooled, reaching ~2.8°C in 2008. Observations at sections crossing the continental slope in the vicinity of Severnaya Zemlya also revealed cooling of AWCT by approximately 0.5°C (Fig. 5.7). This cooling signal has not reached central parts of the Arctic Ocean and the Beaufort Gyre of the Canada Basin (Proshutinsky et al. 2009). In the Beaufort Gyre region, the AWCT in 2008 was 0.80°–0.90°C, which is 0.10°C above AWCT observed in 2007 and 0.50°C above AWCT from pre-1990s climatology. In spring of 2008, data collected at the NPEO (http://psc.apl.washington.edu/northpole/index.html) indicate that the AWCT increased to nearly 1.4°C, which is about 0.1°C higher than observed in a 2007 survey and about 0.7°C higher than pre-1990s climatology.

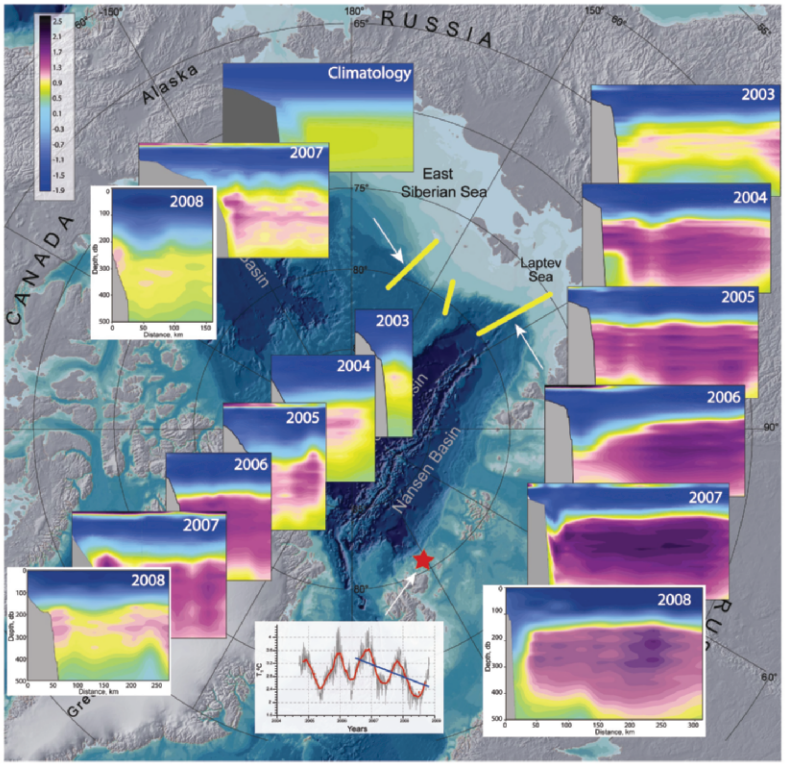

Fig. 5.7. Temporal (°C) and spatial variability of the AWCT. Locations of sections are depicted by yellow thick lines. Mooring location north of Spitsbergen is shown by a red star. There is a decline of Atlantic water temperature at 260 m at mooring locations with a rate of 0.5°C per year starting at the end of 2006. Some cooling in 2008 is also observed at the sections crossing the continental slope in the vicinity of Severnaya Zemlya and in the east Siberian Sea (Polyakov et al. 2009, manuscript submitted to *Geophys. Res. Lett.*).

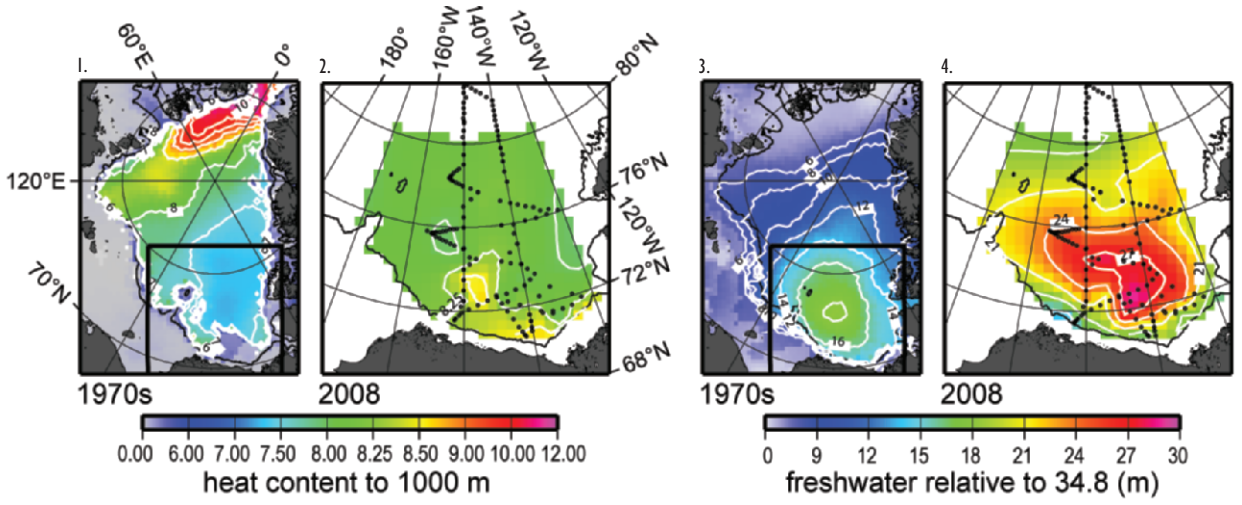

Fig. 5.8. (left) Summer heat (1×10^{10} J m^{-2}) and (right) freshwater (m) content. Panels 1 and 3 show heat and freshwater content in the Arctic Ocean based on 1970s climatology (Arctic Climatology Project 1997, 1998). Panels 2 and 4 show heat and freshwater content in the Beaufort Gyre in 2008 based on hydrographic survey (black dots depict locations of hydrographic stations). For reference, this region is outlined in black in panels 1 and 3. The heat content is calculated relatively to water temperature freezing point in the upper 1000-m ocean layer. The freshwater content is calculated relative to a reference salinity of 34.8.

Summer 2008 ship-based hydrographic surveys (Ashik, Sokolov, Frolov, and Polyakov 2008, personal communications) in different regions of the Arctic Ocean showed a continued freshening of the upper 20-m ocean layer, similar to 2007. In the 25–75-m layer, some salinification was observed in the central regions of Amundsen and Makarov Basins, while along the continental slope the water salinity remained unchanged relative to salinities observed in 2007. There was also some freshening of the deeper water layers in the Beaufort Gyre in 2008, as the surface freshening in this region was accompanied by Ekman pumping (Proshutinsky et al. 2009).

Data collected as part of the BGOS (www.whoi.edu/beaufortgyre/index.html) show that in 2000–08 the total freshwater summer content in the Beaufort Gyre has significantly increased relative to climatology of the 1970s (Arctic Climatology Project 1997, 1998; Fig. 5.8). In 2008, the center of the freshwater maximum remained shifted toward Canada as in 2007 but significantly intensified relative to 2007 (Fig. 5.8). As a result, the northwest part of the region is much saltier and the southeast region of the Beaufort Gyre is much fresher than in 2006–07 and, also, compared to 30 years ago. At some stations in the southeast of the Canada Basin the FWC reached the maximum observed value, increasing by as much as 11 m, which is 60% above climatology values. The freshening extends northward through the Canada and Makarov Basins to the Lomonosov Ridge (not shown). On the Eurasian side of the Lomonosov Ridge, the FWC anomaly is negative (water salinity was increased relative to climatology) with minimum FWC values of about −4 m (McPhee et al. 2009). The Beaufort Gyre heat content is significantly elevated relative to 1970s climatology (Arctic Climatology Project 1997, 1998; Fig. 5.8), but no significant changes relative to 2007 heat content were registered by the BGOS in 2008.

The Bering Strait is an important gateway to the Arctic Ocean. Preliminary observations from a mooring site, established and maintained since 1990 (Woodgate et al. 2006), suggest the 2007 annual mean transport through the Bering Strait is around 1 Sv (1 Sv = 10^6 m^3 s^{-1}), greater than 2006 but comparable with previous high years, such as 2004. The same is true of the freshwater flux through the strait. The heat flux, being largely determined by the total volume flux, is also high, but in this case it appears to be somewhat higher than the 2004 values.

3) Sea Level

Figure 5.9 shows SL time series from nine coastal stations in the Siberian Seas, having representative records for the period of 1954–2008 (Arctic and Antarctic Research Institute data archives). For the nine stations, the rate for 1954–89, after the GIA, was 1.94 ± 0.47 mm yr^{-1}. This compares to an estimated rate of 1.85 ± 0.43 mm yr^{-1} along the Arctic coastlines over the same period, based on 40 arctic coastal stations (Proshutinsky et al. 2004). Addition of 1990–2008 data increases the estimated rate of SL rise for the

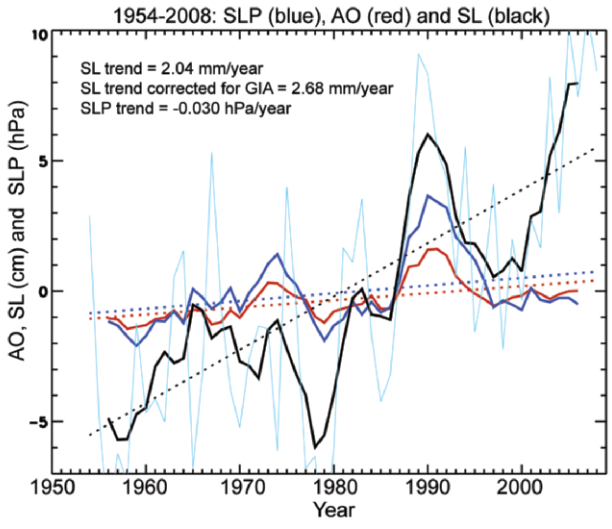

Fig. 5.9. The 5-yr running mean time series: annual mean sea level at nine tide gauge stations located along the Kara, Laptev, east Siberian, and Chukchi Seas' coastlines (black line). The red line is the anomalies of the annual mean AO Index multiplied by 3. The dark blue line is the sea surface atmospheric pressure at the North Pole (from NCAR–NCEP reanalysis data) multiplied by −1. Light blue line depicts annual sea level variability.

nine stations in the Siberian seas, beginning in 1954, to 2.68 ± 0.45 mm yr^{-1} (after correction for GIA).

Until 1996, SL correlates relatively well with the times series of the AO Index and sea level atmospheric pressure at the North Pole (Fig. 5.9). In contrast, from 1997 to 2008 the SL has generally increased, despite the more or less stable behavior of AO and SLP. Possible reasons for the rapidly rising sea level are ocean expansion, due to heating and freshening of the Arctic Ocean, and increased rates of the Greenland ice sheet melt (see section 5f).

d. Sea-ice cover—D. K. Perovich, W. Meier, and S. V. Nghiem

1) Sea-ice extent

Sea-ice extent has become the primary parameter for summarizing the state of the Arctic sea-ice cover. Microwave satellites have routinely and accurately monitored the extent since 1979. There are two periods that define the annual cycle and are thus of particular interest: March, at the end of winter when the ice is at its maximum extent, and September, when it reaches its annual minimum. Maps of ice coverage in March 2008 and September 2008 are presented in Fig. 5.10. The magenta line in the maps denotes the median ice extent for the period 1979–2000. The total area coverage in March was 15.2 million km^2, only 4% less that the 1979–2000 average of 15.8 million km^2. The area of reduced winter ice extent was located largely in the Barents Sea and the Sea of Ohkotsh. The 2008 September summer minimum ice extent was 4.5 million km^2 and was not a record minimum. However, it was the second-lowest ice extent on record, only 0.3 million km^2 greater than 2007 and 36% below the 1979–2000 average. The largest retreats in September 2008 were found in the Beaufort and east Siberian Seas.

The time series of the anomalies in sea-ice extent in March and September for the period 1979–2008, computed with respect to the average from 1979 to 2000, are plotted in Fig. 5.11. The large interannual variability in September ice extent is evident. Both winter and summer ice extent exhibit a negative (decreasing) trend, with values of –2.8% per decade for March and –11.1% per decade for September.

2) Sea-ice age and thickness

The age of the ice is another key descriptor of the state of the sea-ice cover, since older ice tends to be

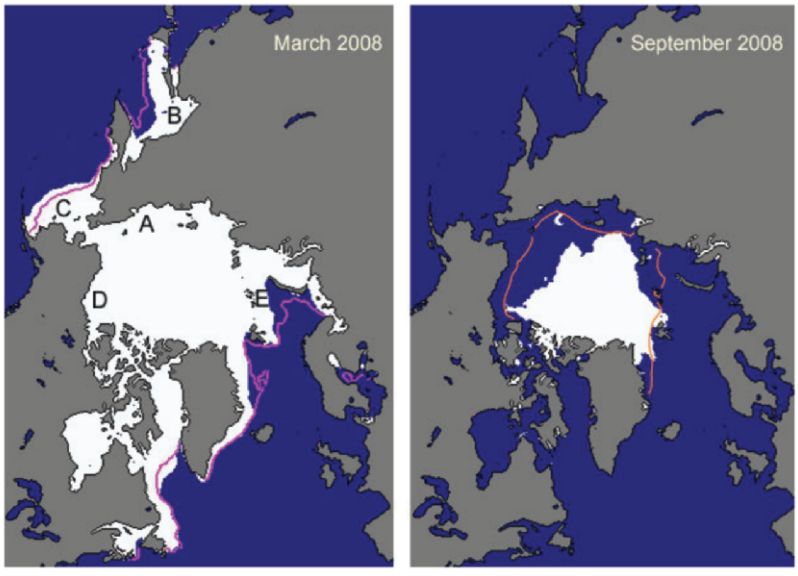

Fig. 5.10. Sea-ice extent in (left) Mar 2008 and (right) Sep 2008, illustrating the respective winter maximum and summer minimum extents. The magenta line indicates the median maximum and minimum extent of the ice cover, for the period 1979–2000. A—east Siberian Sea, B—Sea of Ohkotsh, C—Bering Sea, D—Beaufort Sea, and E—Barent's Sea. (Figures from the NSIDC Index: nsidc.org/data/seaice_index.)

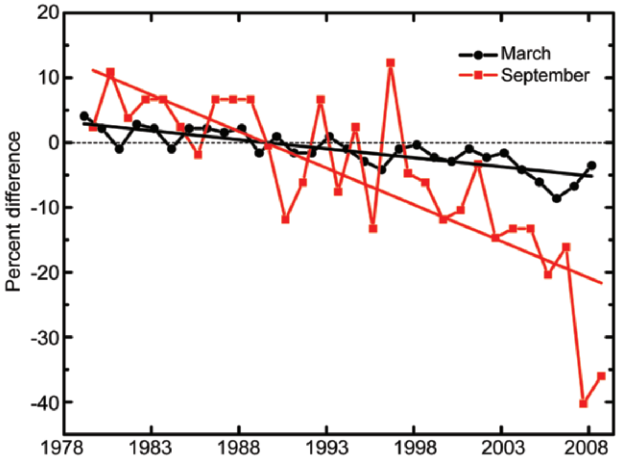

Fig. 5.11. Time series of the percent difference in ice extent in Mar (the month of ice-extent maximum) and Sep (the month of ice-extent minimum) from the mean values for the period 1979–2000. Based on a least-squares linear regression, the rate of decrease for the Mar and Sep ice extents was −2.8% and −11.1% per decade, respectively.

thicker and more resilient than younger ice. A simple two-stage approach classifies sea ice as seasonal or perennial. Seasonal ice freezes in the winter and melts in the summer, while perennial ice can last for several years. Satellite-derived maps of ice age for March and September in 2007 and 2008 are presented in Fig. 5.12.

QuikSCAT data show the Arctic perennial sea-ice extent on 1 March 2008. A combination of the satellite and surface drift data records (Rigor and Wallace 2004) confirmed that the 2008 winter perennial ice extent was a minimum compared to data over the last half-century. The extent of perennial sea ice on 1 March 2008 was reduced by 1 million km^2 compared to that at the same time last year (Fig. 5.12, top). This decrease of perennial ice continues a decade-long sharp decline, caused in part by enhanced wind-driven transport of perennial ice out of the Arctic Basin via the Fram and Nares Straits (Nghiem et al. 2006, 2007).

A noteworthy, albeit explicable, aspect of the 2008 summer melt season was the higher-than-average retention of first-year sea ice, with much more first-year ice surviving in 2008 than in 2007 (Fig. 5.12, bottom). This observation is counterintuitive because relatively thin first-year ice is typically prone to complete melting. One cause of the large first-year ice survival rate was that early summer 2008 was cooler than in 2007 and the lower air temperatures slowed the melt rate in the early part of the season (NSIDC, http://nsidc.org/news/press/20081002_seaice_pressrelease.html). Conditions in August favored rapid ice loss, but this did not make up for the modest early season melt. Furthermore, much of this year's first-year ice was located at higher latitudes than in 2007, covering even the geographic North Pole. These far north regions receive less solar energy and have less melting.

The total volume of sea ice depends on the ice area and the ice thickness. Unfortunately, ice thickness is difficult to monitor. Surface-based measurements are few in number and submarine observations are at irregular temporal spacing. Satellite-based techniques (Laxon et al. 2003; Kwok et al. 2004, 2007) offer the promise of complete spatial and temporal coverage but are not yet fully operational. Thickness data from these various sources indicate a net thinning of the Arctic sea-ice cover. Submarine-based observations indicate that over the period 1975 to 2000, the annual mean thickness of the ice cover declined

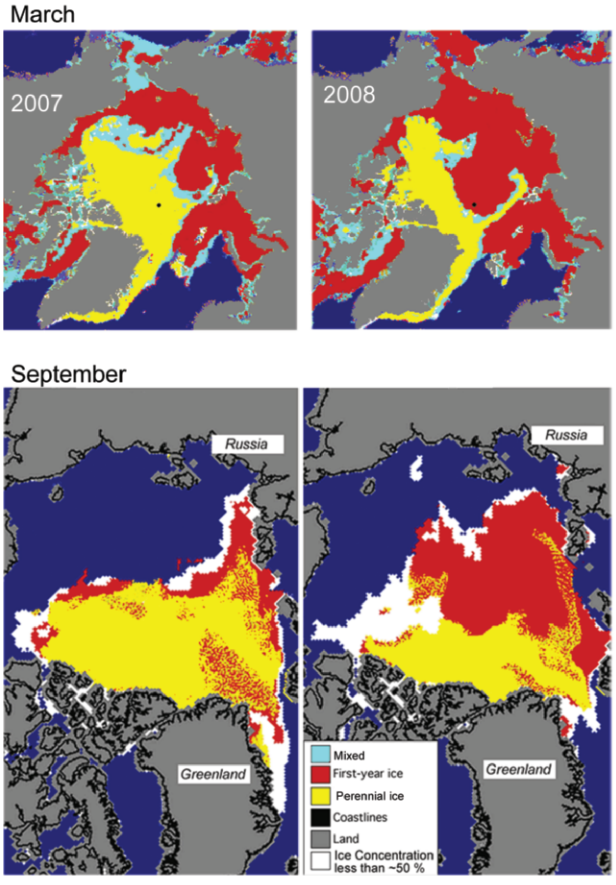

Fig. 5.12. Maps of age of Arctic sea ice for (left) 2007 and (right) 2008 in (top) Mar and (bottom) Sep. (top) Derived from QuikSCAT data (Nghiem et al. 2007). (bottom) Courtesy of C. Fowler, J. Maslanik, and S. Drobot, NSIDC, and are derived from a combination of AVHRR and SSM/I satellite observations and results from drifting ice buoys.

from 3.71 m in 1980 to 2.46 m in 2000, a decrease of 1.25 m (Rothrock et al. 2008). Maslanik et al. (2007) generated a proxy ice-thickness record for 1982–2007 by combining satellite estimates of sea-ice age and thickness, and the record indicates significant thinning between 1982 and 2007. A reduction of modal and mean sea ice thicknesses in the region of the North Pole of up to 53% and 44%, between 2001 and 2007, has been observed by Haas et al. (2008) using helicopter-borne electromagnetic ice-thickness profilers. Using satellite radar altimetry data, covering the Arctic Ocean up to 81.5°N, Giles et al. (2008) observed that after the melt season of 2007, the average sea-ice thickness was 0.26 m below the 2002/03 to 2007/08 average. In contrast to the central Arctic, measurements of the seasonal and coastal ice cover do not indicate any statistically significant change in thickness in recent decades (Melling et al. 2005; Haas 2004; Polyakov et al. 2003), indicating that the thinning of the ice cover is primarily the result of changes in perennial ice thickness.

e. *Land*—D. A. Walker, U. S. Bhatt, M. K. Raynolds, J. E. Comiso, H. E. Epstein, and G. J. Jia

1) Vegetation

Models have predicted that the retreating sea ice (see section 5d) should affect the temperature and ecosystems of adjacent lands (e.g., Lawrence et al. 2008). Time series of sea-ice area and land temperatures, as well as an index of greening, were investigated for trends and variability during the period 1982–2007 along the coastlines of 14 Arctic seas (Fig. 5.13). Temporal analyses of these regional time series (not shown) consistently indicate that higher land-surface temperatures and higher NDVI values correspond to below-average sea-ice concentration (Bhatt et al. 2008, 2009, manuscript submitted to *Earth Interactions*).

The trend analysis shows that coastal sea ice declined in all regions, with a decrease of 25% for the Northern Hemisphere as a whole (Fig. 5.13, top blue bar). The largest declines were along the northern Beringia region, including the west Chukchi, east Chukchi, and east Siberia Seas. This portion of the Arctic saw large areas of summer ice retreat in 2005 and 2007.

Land temperatures as measured by the summer warmth index (sum of the monthly mean temperatures that are above freezing) increased 24% for the Northern Hemisphere as a whole (Fig. 5.13, top red bar). However, the coastal areas of the North America Arctic have experienced a 27% increase in land temperatures, while Eurasia experienced only a 16% increase. The largest increases occurred in the Beringia region (east Siberia, west Chukchi, west Bering, and east Chukchi) and in the Greenland and Baffin Island regions (Greenland Sea, Baffin Bay, and Davis Strait). The smallest increases were seen along

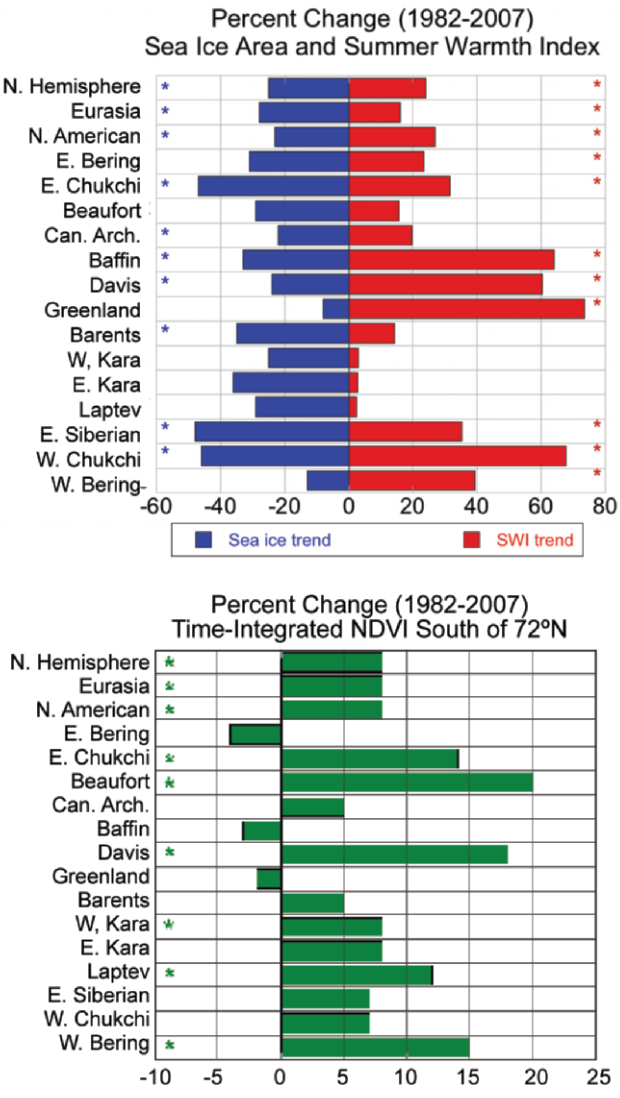

Fig. 5.13. (top, blue bars) Percentage change in sea-ice area in late spring (when the long-term mean 50% concentration is reached) during 1982–2007 along the 50-km-seaward coastal margin in each of the major seas of the Arctic using 25-km-resolution SSMI passive microwave Bootstrap sea-ice concentration data (Comiso and Nishio 2008). (top, red bars) Percentage change in the summer land-surface temperature along the 50-km-landward coastal margin as measured by the SWI [sum of the monthly mean temperatures above freezing (°C mo)] based on AVHRR surface-temperature data (Comiso 2003). (bottom, green bars) Percentage change in greenness for the full tundra area south of 72°N as measured by the TI-NDVI based on biweekly GIMMS NDVI (Tucker et al. 2001). Asterisks denote significant trends at $p < 0.05$. Based on Bhatt et al. (2008).

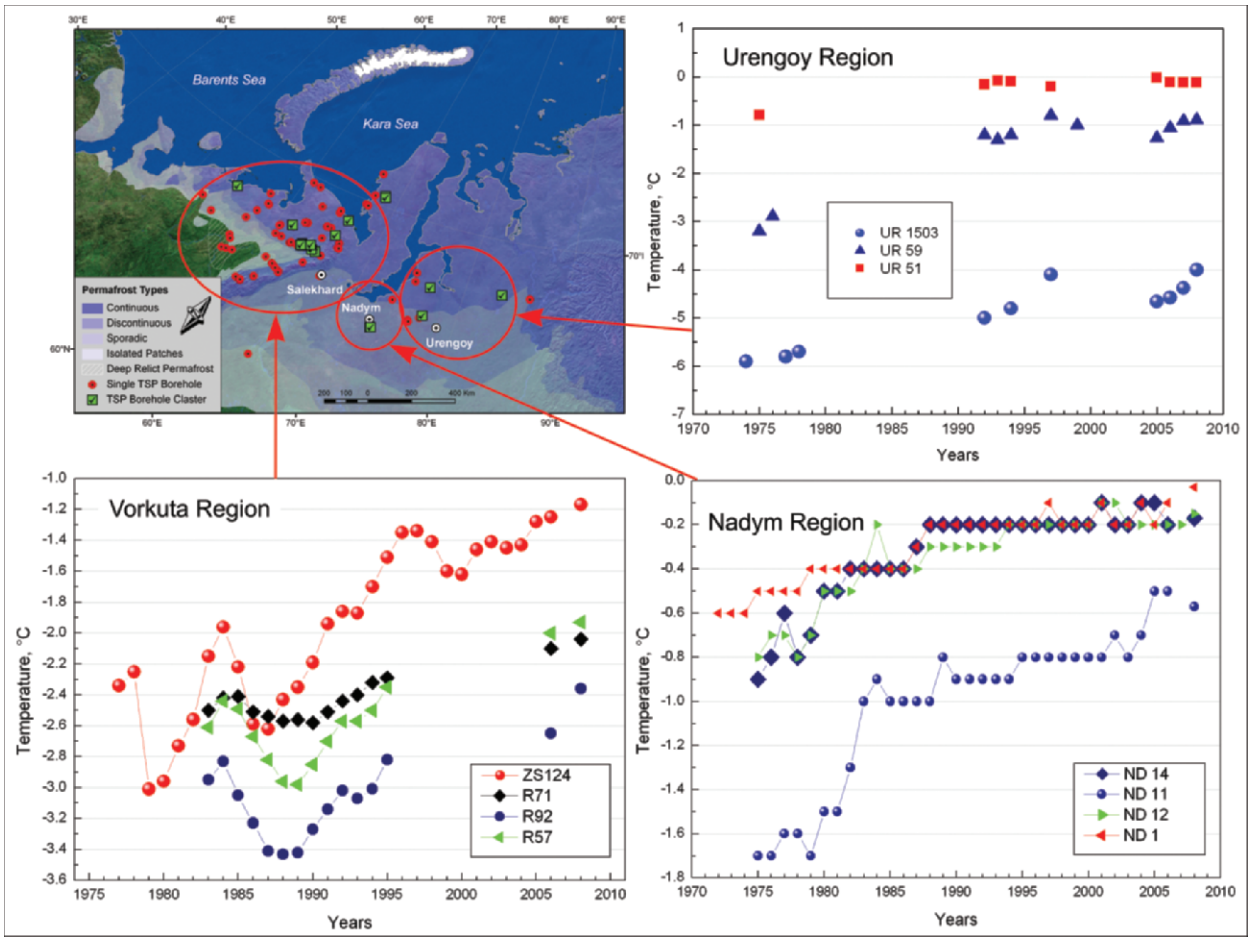

Fig. 5.14. (top left) Location of the long-term MIREKO and the Earth Cryosphere Institute permafrost observatories in northern Russia. (bottom left) Changes in permafrost temperatures at 15-m depth during the last 20 to 25 years at selected stations in the Vorkuta region (updated from Oberman 2008). (top right) Changes in permafrost temperatures at 10-m depth during the last 35 yr at selected stations in the Urengoy and Nadym (bottom right) regions (updated from Romanovsky et al. 2008).

the northern coast of Russia (Laptev Sea, east Kara Sea, and west Kara Sea).

Greenness was determined using the TI-NDVI derived from the GIMMS data. TI-NDVI is an index of the productivity of the vegetation each summer that is derived from Earth's reflectance in the visible and near-infrared portions of the spectrum. The TI-NDVI analysis was limited to the area south of 72°N (covers primarily the low Arctic) because of a discontinuity in the GIMMS data at this latitude. TI-NDVI increased 8% for the Arctic as a whole (Fig. 5.13, top green bar) but was variable. The largest increase was along the Beaufort Sea coast (20%). Other large increases occurred adjacent to the Davis Strait and the east Chukchi and west Bering Seas. Smaller increases occurred in much of northern Russia (Barents, Kara, east Siberian, and west Chukchi Seas), generally where summer temperature increases were lower. A few nonsignificant negative trends occurred in the east Bering Sea, Baffin Bay, and Greenland Sea. The NDVI changes noted here are in general agreement with other analyses of NDVI trends in the Arctic (Jia et al. 2003; Goetz et al. 2005; Verbyla 2008; Raynolds et al. 2008) and ground observations (Tape et al. 2006; Walker et al. 2008; Epstein et al. 2008).

2) Permafrost—V. Romanovsky, N. Oberman, D. Drozdov, G. Malkova, A. Kholodov, and S. Marchenko

Observations show a general increase in permafrost temperatures during the last several decades in Alaska (Romanovsky et al. 2002, 2007; Osterkamp 2008), northwest Canada (Couture et al. 2003; Smith et al. 2005), Siberia (Oberman and Mazhitova 2001; Oberman 2008; Drozdov et al. 2008; Romanovsky et al. 2008), and northern Europe (Isaksen et al. 2000; Harris and Haeberli 2003).

Most of the permafrost observatories in Alaska show a substantial warming during the last 20 years.

The detailed characteristic of the warming varies between locations, but it is typically from 0.5° to 2°C at the depth of zero seasonal temperature variations in permafrost (Osterkamp 2008). It is worth noting that permafrost temperature has been relatively stable on the North Slope of Alaska during 2000–08.

Permafrost temperature has increased by 1° to 2°C in northern Russia during the last 30 to 35 years (Fig. 5.14). This increase is very similar in magnitude and timing to what has been observed in Alaska. Also, a common feature for Alaskan and Russian sites is more significant warming in relatively cold permafrost than in warm permafrost. An especially noticeable permafrost temperature increase in the Russian Arctic was observed during the last two years. The mean annual permafrost temperature at a 15-m depth increased by more than 0.3°C in the Tiksi area and by 0.25°C at a 10-m depth in the European north of Russia.

The last 30 years of generally increasing permafrost temperatures have resulted in thawing of permafrost in areas of discontinuous permafrost in Russia (Oberman 2008). At one of the locations, the upper boundary of permafrost lowered to 8.6 m in 30 years. It lowered even more, to almost 16 m, in an area where a newly developed talik (a volume or layer of all-year-round unfrozen soil above or within the permafrost) coalesced with an already existing lateral talik. The average increase in depth of the permafrost table in the Vorkuta and Nadym regions in Russia ranged from 0.6 to 6.7 m, depending on the geographical location, ice content, lithological characteristics of sediments, hydrological, hydrogeological, and other factors.

3) River discharge—A. Shiklomanov

A general increase of river discharge to the Arctic Ocean from Eurasia was observed over the period 1936–2007, with a rate of annual change (defined from the linear trend) of 2.7 ± 0.5 km^3 yr^{-1} (Fig. 5.15). The most pronounced positive (increasing) trend for the six largest Eurasian rivers is observed during the last 21 years (1987–2007), at a rate of 11.8 km^3 yr^{-1}. The rate of discharge has continued to increase in the twenty-first century. The mean 2000–07 discharge was 171 km^3 higher (10%) than the long-term average over the period 1936–99. A new historical maximum for Eurasian river discharge to the Arctic Ocean was observed in 2007, reaching 2250 km^3 yr^{-1} or 30% higher than the long-term mean discharge from 1936–99, reported in Peterson et al. (2002).

The mean annual discharge to the ocean over 2000–07 from the five large North American Arctic rivers, based on data from the Environment Canada and USGS, was about 6% (31 km^3) greater than the long-term mean from 1973 to 1999. The river discharge during 2007 was higher than the long-term mean and, taking into account that this year had extremely high freshwater discharge from Greenland (Mernild et al. 2009), we can estimate that 2007 showed record-high total freshwater input to the Arctic Ocean from the terrestrial land surface.

Provisional estimates, made using techniques developed by Shiklomanov et al. (2006), indicate that the 2008 annual river discharge to the Arctic Ocean from the Russian rivers was significantly greater than the long-term mean but lower than the historical maximum observed in 2007 (Fig. 5.15).

4) Terrestrial snow—C. Derksen, R. Brown, and L. Wang

The 2007/08 Arctic snow season was characterized by close-to-normal snow cover onset over North America and Eurasia, with above-normal seasonal accumulation over Siberia and much of North America. The Arctic spring melt was characterized by close-to-normal conditions over Eurasia, but the earliest snow cover disappearance in the period of record (1966–present) over North America.

Various satellite and conventional measurements provide a comprehensive perspective on terrestrial snow including SCD, SD, and melt timing/duration (Brasnett 1999; Brown et al. 2007; Helfrich et al. 2007;

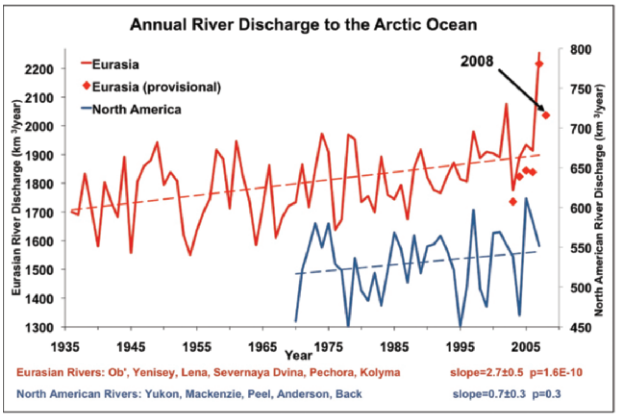

Fig. 5.15. Total annual river discharge to the Arctic Ocean from the six largest rivers in the Eurasian Arctic for the observational period 1936–2007 (updated from Peterson et al. 2002) (red line) and from the five large North American pan-Arctic rivers over 1973–2006 (blue line). The least-squares linear trend lines are shown as dashed lines. Provisional estimates of annual discharge for the six major Eurasian Arctic rivers, based on near-real-time data from http://RIMS.unh.edu, are shown as red diamonds.

Wang et al. 2008a). SCD anomalies for the 2007/08 snow season, derived from NOAA weekly snow charts (available online at climate.rutgers.edu/snowcover/), illustrate a reduced snow cover season over the eastern Canadian Arctic, most of Europe, and eastern Siberia, compared to a longer-than-normal snow season in central China and the midlatitudes of North America (Fig. 5.16a). The period 1988–2007 is selected as the historical reference period for this assessment to place anomalies in the context of more recent snow cover conditions following a rapid reduction in hemispheric snow cover during the 1980s. Time series of SCD anomalies across the North American and Eurasian sectors of the Arctic (north of 60°N) are illustrated in Fig. 5.16b. SCD anomalies are generally in-phase for both sectors, with the 2007/08 snow cover season close to the 1988–2007 normal for snow cover onset (fall SCD). For snowmelt (spring SCD) the Eurasian average was close to normal, while the North American Arctic had the earliest disappearance of snow in the NOAA record (since 1966). This is a continuation of shorter snow seasons observed since the rapid reductions in the 1980s. Unlike summer sea-ice concentration, however, there is no linear decrease in Arctic spring SCD over the past decade.

Annual maximum SD anomalies for 2007/08 (1998–2008 reference period), determined from the CMC analysis (Brasnett 1999), are shown in Fig. 5.16c. Over Siberia, positive SD anomalies coincide with below-normal SCD, indicating above-average snowfall but early spring melt—a continuation of recent trends reported in Kitaev et al. (2005).

The main melt onset date for 2008 across the pan-Arctic land mass was derived from Ku-band scatterometer measurements available from QuikSCAT using the algorithm of Wang et al. (2008a). The melt onset anomaly relative to the 9-yr QuikSCAT record (2000 to 2008) confirms regional early melt onset over the North American Arctic that agrees with early dates of snow disappearance identified from the NOAA record (Fig. 5.16d). In the Eurasian region there was a pattern of generally late melt onset between approximately 60°–65°N, anomalously early melt across 65°–70°N, and then a transition to late melt onset again across the northern portion of Eurasia.

5) Glaciers outside Greenland—M. Sharp and G. Wolken (with acknowledge data contributions from D. Burgess, G. Cogley, P. Glowacki, J. Jania, S. O'Neel, D. Puczko, A. Arendt, and S. Luthcke)

Glacier shrinkage is a major contributor to global sea level change (Meier et al. 2007). Surface mass

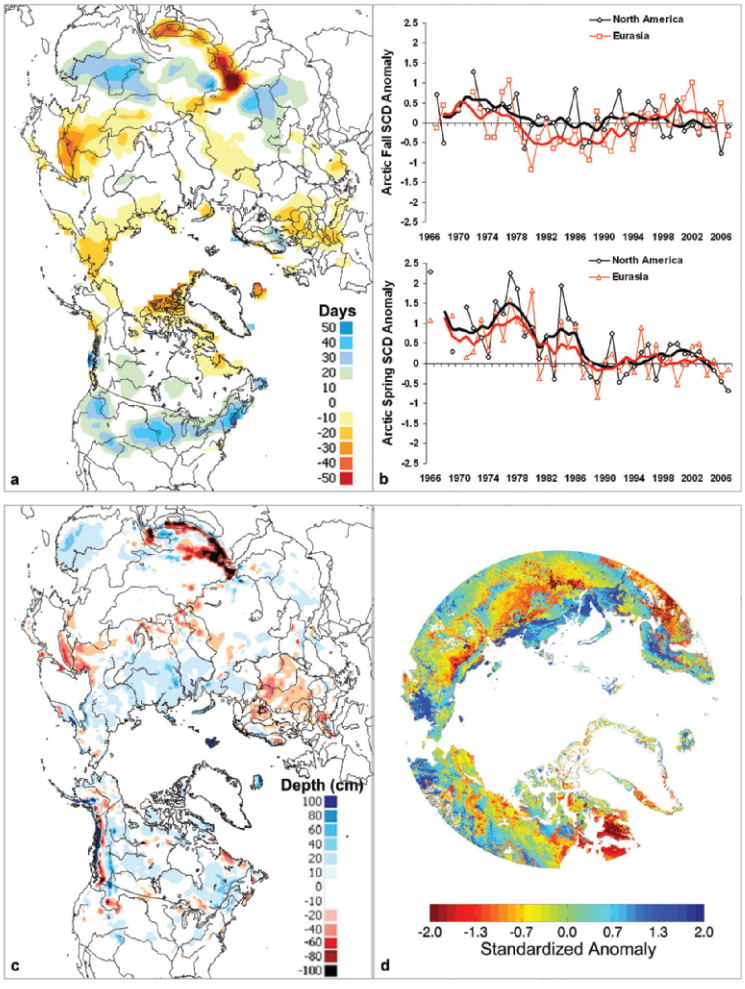

Fig. 5.16. (a) SCD anomalies (with respect to 1988–2007) for the 2007/08 snow year and (b) Arctic seasonal SCD anomaly time series (with respect to 1988–2007) from the NOAA record for the first (fall) and second (spring) halves of the snow season. Solid lines denote 5-yr moving average. (c) Maximum seasonal snow depth anomaly for 2007/08 (with respect to 1998/99–2007/08) from the CMC snow depth analysis. (d) Terrestrial snowmelt onset anomalies (with respect to 2000–08) from QuikSCAT data derived using the algorithm of Wang et al. (2008a). The standardized anomaly scales the date of onset of snowmelt based on the average and the magnitude of the interannual variability in the date at each location. A negative anomaly (shown in red-yellow) indicates earlier onset of snowmelt in the spring.

balance (annual net balance and its summer/winter components) measures how climate affects the health of Arctic glaciers. As most 2007–08 measurements are not yet available, we report results for the 2006–07 balance year (Svalbard: 4 glaciers, Iceland: 6, Alaska: 3, Arctic Canada: 4). Annual surface balances were negative for 14 glaciers, positive for 2 (1 each in Iceland and Alaska), and zero for 1 (in Svalbard) (WGMS 2009).

Summer (JJA 2008) 700-hPa air temperature and winter (September 2007–May 2008) precipitation data from the NCEP–NCAR reanalysis serve as climatic indices for regions centered over each of the Arctic's major glaciated regions (excluding Greenland) (Table 5.1). Sixteen discrete regions form four groups (Alaska, Arctic Canada, Iceland, and the Eurasian Arctic) based on correlations between 1948 and 2008 NCEP summer temperature series. These indices suggest that the 2008 annual mass balance was likely extremely negative in Arctic Canada, due to unusually high summer air temperatures, and positive in Alaska due to strong positive winter precipitation anomalies (confirmed by GRACE satellite gravimetry; S. Luthcke 2009, personal communication). Annual balance was likely near zero or slightly positive in the Eurasian Arctic (relatively cool summers and generally high winter precipitation) and negative in Iceland (higher-than-average summer temperatures and below-average winter precipitation).

Melt onset and freeze-up dates and 2008 melt season duration were determined from temporal backscatter variations measured by QuikSCAT's SeaWinds (Table 5.1). In Arctic Canada, melt duration anomalies (relative to 2000–04 climatology) on the North Ellesmere, Agassiz, and Axel Heiberg ice caps ranged from +17.6 to +22.5 days, largely due to late freeze-up. Here, summer 2008 was the longest melt season in the 2000–08 record. Melt duration anomalies were also strongly positive on northern Prince of Wales Icefield and Severnaya Zemlya, and positive in central and southern Arctic Canada, Franz Josef Land, and Iceland. The melt season in southwest Alaska was the shortest in the 9-yr record, with strongly negative melt duration anomalies, mostly due to early freeze-up.

The total ice shelf area in Arctic Canada decreased by 23% in summer 2008 (Mueller et al. 2008). The Markham ice shelf disappeared completely and the Serson ice shelf lost 60% of its area. In the past century, 90% of the Arctic ice shelf area has been lost. Several fjords on the north coast of Ellesmere Island are now ice free for the first time in 3,000–5,500 years (England et al. 2008).

f. Greenland—J. E. Box, L.-S. Bail, R. Benson, I. Bhattacharya, D. H. Bromwich, J. Cappelen, D. Decker, N. DiGirolamo, X. Fettweis, D. Hall, E. Hanna, T. Mote, M. Tedesco, R. van de Wal, and M. van den Broeke

1) Summary

An abnormally cold winter across the southern half of Greenland led to substantially higher west coast sea ice thickness and concentration. Even so, record-setting summer temperatures around Greenland, combined with an intense melt season (particularly across the northern ice sheet), led the 2008 Greenland climate to be marked by continued ice sheet mass deficit and floating ice disintegration.

2) Regional surface temperatures

Temperature anomalies were mixed and exhibited seasonal variability (Fig. 5.17). Annual mean temperatures for the whole ice sheet were +0.9°C, but were not abnormal, given a rank of 23 of 51 years over the 1958–2008 period (Box et al. 2006). Persistent warm anomalies were evident over the northern ice sheet in all seasons. Temperatures were abnormally cold over the southern ice sheet in winter. Coastal meteorological stations around Greenland with a consistent 51-yr period (1958–2008) (Cappelen 2009) indicate a record-setting warm summer in 2008. The Upernavik (Nuuk) summer temperature was the warmest (second warmest) on record since 1873, respectively.

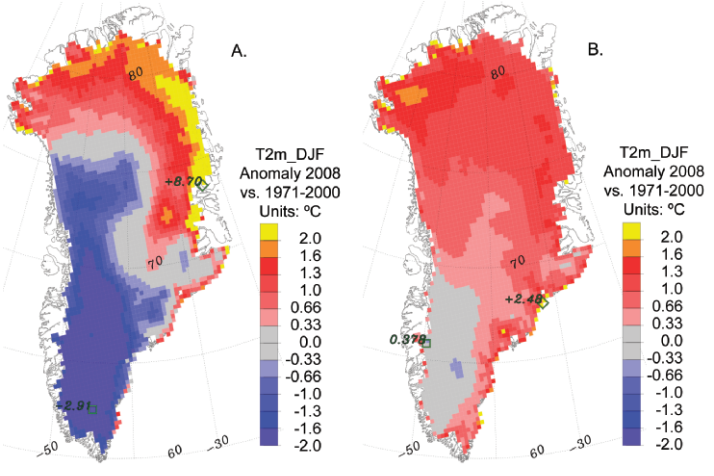

Fig. 5.17. 2008 (a) winter and (b) summer near-surface (2 m) air temperature anomalies with respect to the 1971–2000 base period, simulated by Polar MM5 after Box et al. (2006).

Table 5.1. 2008 Summer 700-hPa temperature and winter precipitation anomalies (relative to 1948–2008 NCEP reanalysis means) for glaciated regions of the Arctic (excluding Greenland). Inferred sign of surface mass balance is based on comparison of historical mass balance records for each region with NCEP reanalysis temperature and precipitation anomalies. Anomalies in melt duration and the timing of melt onset and freeze-up (relative to 2000–04 climatology) derived from QuikSCAT data. For timing, negative anomalies indicate an earlier-than-normal date.

Region	Sub-region	Latitude (°N)	Longitude (°E)	JJA 700-hPa T Anomaly	2008 Rank	Sep–May Ppt Anomaly	2008 Rank	Inferred Surface Balance	Melt Onset Anomaly	Freeze-up Anomaly	Melt Duration Anomaly
				(°C)	(*N* = 60)	(mm)	(*N* = 60)		days	days	days
Arctic Canda	North Ellesmere Island	80.6–83.1	267.7–294.1	2	4	12.3	10	−−	−1.8	9.8	19.3
	Axel Heiberg Island	78.4–80.6	265.5–271.5	1.67	5	0	30	−−	−2.9	11.4	17.6
	Agassiz Ice Cap	79.2–81.1	278.9–290.4	2.11	3	−9.2	44	−−	5.4	24.0	22.5
	Prince of Wales Icefield	77.3–79.1	278–284.9	1.77	7	−11.4	42	−−	2.1	7.8	10.2
	Sydkap	76.5–77.1	20.7–275.8	1.53	6	−58.5	59	−−	3.0	3.8	1.4
	Manson Icefield	76.2–77.2	278.7–282.1	1.71	7	−62.5	56	−−	6.4	5.7	0.0
	Devon Ice Cap	74.5–75.8	273.4–280.3	1.47	6	−8	33	−−	0.8	−0.8	5.8
	North Baffin	68–74	278–295	1.97	2	12.4	17	−−	−26.9	−14.4	4.9
	South Baffin	65–68	290–300	2.39	1	5.9	25	−−	−2.8	−1.6	−1.1
Eurasian Arctic	Severnaya Zemlya	76.25–81.25	88.75–111.25	−0.36	41	38.9	17	+	−0.2	13.4	10.6
	Novaya Zemlya	68.75–78.75	48.75–71.25	0.29	24	78	6	+	21.5	−5.3	−4.2
	Franz Josef Land	80–83	45–65	−0.77	46	110	3	++	8.4	−2.4	6.1
	Svalbard	76.25–81.25	8.75–31.25	0.13	31	58.5	7	+	−6.6	−2.8	−0.8
Iceland		63–66	338–346	0.13	27	−29.3	46	−	−4.2	−14.4	6.5
Alaska	SW Alaska	60–65	210–220	−0.33	40	117.4	14	+	3.5	−15.6	−17.7
	SE Alaska	55–60	220–230	−0.91	50	237	5	++	*	*	*

3) Upper-air temperatures

Upper-air sounding data available from the Integrated Global Radiosonde Archive (Durre et al. 2006) indicate a continued pattern of lower tropospheric warming and lower stratospheric cooling 1964-onward (Box and Cohen 2006). Lower tropo-

spheric warm anomalies in all seasons, particularly in spring along western Greenland, were accompanied by relatively small midtropospheric cool anomalies. Winter tropopause temperatures (200 hPa) were above normal. Lower stratospheric (above 100 hPa) temperatures were lower than normal.

4) Surface melt extent and duration

Passive (SMMR and SSM/I, 1979–2008) and active (QuikSCAT, 2000–08) microwave remote sensing (Bhattacharya et al. 2009, submitted to *Geophys. Res. Lett.*; Liu et al. 2005) indicate abnormally high melt duration over the north and northeast ice sheet and along the east and west coasts above Greenland's most productive three outlet glaciers in terms of ice discharge into the sea: Kangerlussuaq; Helheim; and Jakobshavn (Fig. 5.18). Lower-than-normal melt duration is evident over much of the upper elevations of the ice sheet. New records of the number of melting days were observed over the northern ice sheet, where melting lasted up to 18 days longer than previous maximum values. Anomalies near the west coast are characterized by melting up to 5–10 days longer than the average (Tedesco et al. 2008).

The average daily melt extent, after Mote and Anderson (1995) and Mote (2007), for 2008 was 424,000 km^2, about 2.4% greater than the 1989–2008 average of 414,000 km^2, representing the lowest average melt extent since 2001. Significantly more melt occurred in 2008 in the northeast (45.6% greater than the 1989–2008 average) and northwest (29.7%), but less occurred in the two east-central regions (–16.8% and –25.4%) and in the southeast (–21.1%). Melt extent in 2008 was also above the 1979–2007 average. The trend in the total area of melt during 1979–2008 is approximately +15,900 km^2 yr^{-1} and is significant at the 95% confidence interval ($p < 0.01$).

5) Precipitation anomalies

Annual PT anomalies in 2008, determined using Polar MM5 data assimilation modeling (Bromwich et al. 2001; Cassano et al. 2001; Box et al. 2006), were positive (negative) up to 750 mm (–250 mm) over the eastern (western) ice sheet, respectively. More PT than normal occurred in isolated areas in extreme southeast, east, north, and northwestern Greenland. The overall anomaly indicated approximately 41 Gt more PT than normal for the 1971–2000 standard normal period.

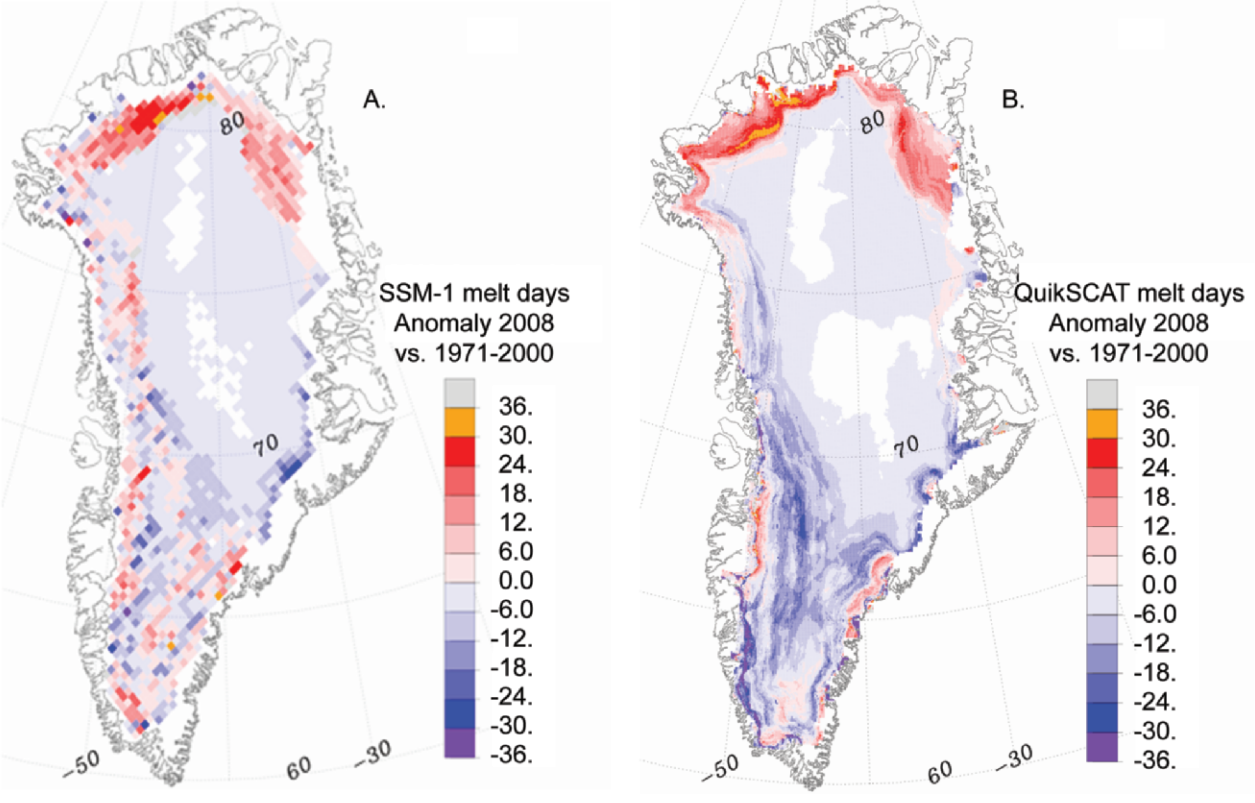

Fig. 5.18. 2008 Greenland ice sheet surface melt duration anomalies relative to the 1989–2008 base period based on (a) SSM/I and (b) QuikSCAT (2000–08 base period), after Bhattacharya et al. (2009, submitted to *Geophys. Res. Lett.*).

Table 5.2. Greenland ice sheet surface mass balance parameters: 2008 departures from 1971–2000 average (adapted from Box et al. 2006). Estimates by Hanna et al. (2008) are included for comparison.

	Box			Hanna		
	Mean (1971–2000)	% of normal	2008 Anomaly (Gt)	Mean (1971–2000)	% of normal	2008 Anomaly (Gt)
Total Precipitation	710.7	105%	38.5	624.16	108%	52
Liquid Precipitation	16.8	142%	7.1	27.01	147%	13
Surface Water Vapor Flux	66.7	100%	−0.2	40.59	74%	−11
Blowing Snow Sumblimation	39.6	99%	−0.3			
Snow Accumulation	604.5	106%	39.0	556.56	109%	50
Meltwater Volume	330.1	159%	194.1	333.95	133%	110
Meltwater Runoff	214.9	186%	184.3	277.91	142%	116
Surface Mass Balance	389.6	63%	−145.3	305.66	83%	−53
Mean T	−19.0		0.9	−21.4		1.1
AAR	0.920	0.905%	−0.087	0.859	0.933%	−0.007

6) Surface albedo

Melt season (day 92–274) surface albedo anomalies, derived using the Liang et al. (2005) algorithm applied to daily cloud-free MODIS imagery, indicate a lower surface albedo around the ablation zone (except the east ice sheet) (Fig. 5.19) resulting from the combined effect of the positive summer surface melt intensity anomaly and, in most areas, less winter snow coverage. A positive albedo anomaly is evident for the ice sheet accumulation zone and is consistent with above-average solid precipitation and/or less-than-normal melting/snow grain metamorphism.

7) Surface mass balance

Polar MM5 climate data assimilation model runs spanning 51 years (1958–2008), calibrated by independent in situ ice-core observations (Bales et al. 2001; Mosley-Thompson et al. 2001; Hanna et al. 2006) and ablation stakes (van de Wal et al. 2006), indicate that 2008 total precipitation and net snow accumulation was slightly (6%–8%) above normal (Table 5.2). In accordance with a +0.9°C 2008 annual mean surface temperature anomaly, the fraction of precipitation that fell as rain instead of snow, surface meltwater production, and meltwater runoff were 142%–186% of the 1971–2000 mean. Consequently, and despite 6%–9% (39–50 Gt) more snow accumulation than normal, the surface net mass balance was substantially (145 Gt) below normal. 2008 surface mass balance ranked ninth-least positive out of 51 years (1958–2008).

Surface mass balance anomalies indicate a pattern of increased marginal melting with noteworthy departures in excess of 1-m water equivalence per year from normal across the northern ice sheet (Fig. 5.20). The pattern of steepening mass balance profile is consistent with observations from satellite altimetry (Zwally et al. 2005) and airborne altimetry (Krabill et al. 2000); satellite gravity retrievals (e.g., Luthcke et al. 2006); and climate projections (Solomon et al. 2007).

8) Floating glacier ice changes

Daily surveys of Greenland ice sheet marine terminating outlet glaciers from cloud-free MODIS imagery (http://bprc.osu.edu/MODIS/) indicate that the 32 widest glaciers collectively lost 184.1 km^2 of mostly floating ice between the end of summer 2007 and the end of summer 2008. The 2008 area loss was 3 times that of the previous summer (2006–07 area

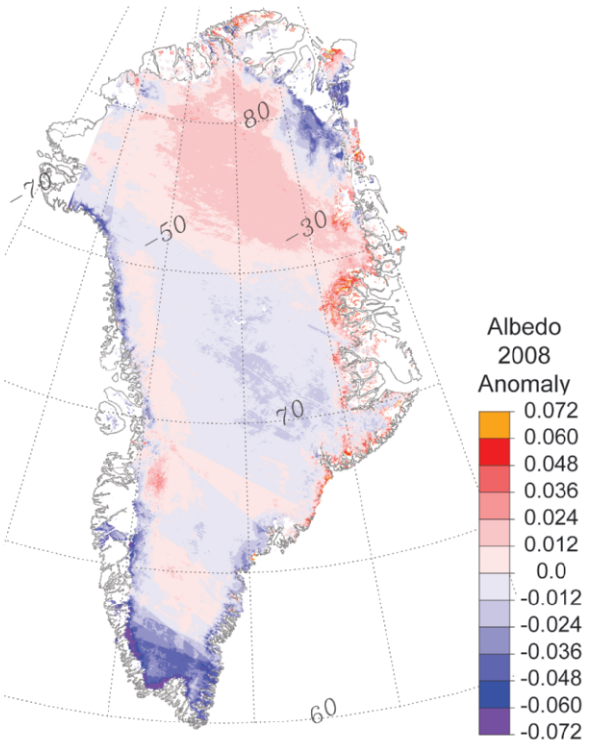

Fig. 5.19. Surface albedo anomaly Jun–Jul 2008 relative to a Jun–Jul 2000–08 base period.

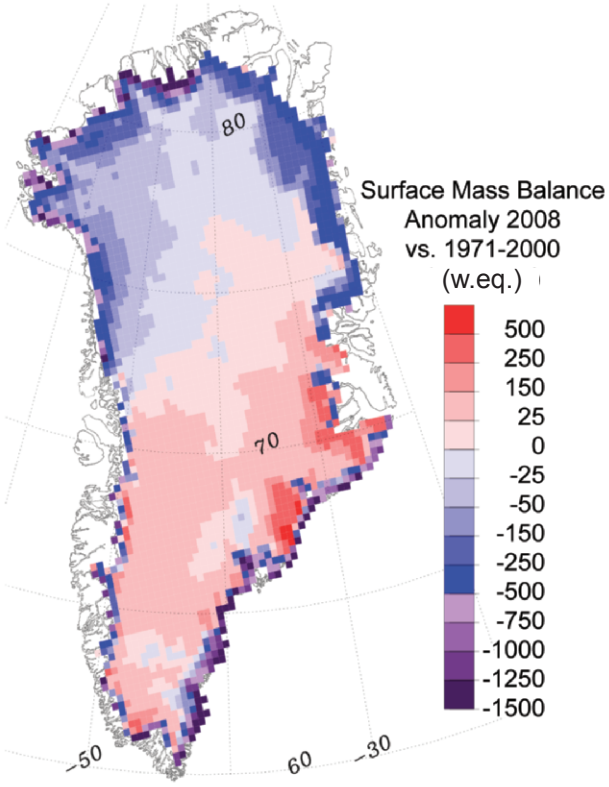

Fig. 5.20. 2008 surface mass balance anomalies with respect to the 1971–2000 base period, simulated by Polar MM5 after Box et al. (2006).

change was −60.8 km^2) and 1.7 times greater than the 8-yr trend, beginning in 2000 when MODIS data became available. In 2008, 18 of the 32 glaciers retreated relative to their end-of-summer 2007 position. The total net effective length change of these glaciers was −9.1 km. These losses marked a continuation of a deglaciation trend of −106.4 km^2 yr^{-1} area change (R = −0.98) since 2000. In other words, between 2007 and 2008, glaciers around Greenland lost an area more than 2 times the size of Manhattan Island, New York. The cumulative area change from end-of-summer 2000 to 2008 is −920.5 km^2, an area loss equivalent to 10 times the area of Manhattan Island.